Available online at www.sciencedirect.com
SCIENCE DIRECT®
International Journal of Heat and Mass Transfer 49 (2006) 3240–3252
International Journal of HEAT and MASS TRANSFER
www.elsevier.com/locate/ijhmt

Steady free convection boundary layer over a vertical flat plate embedded in a porous medium filled with water at 4 °C

V. Kumaran [a,*], I. Pop [b]

[a] Department of Mathematics, National Institute of Technology, Tiruchirappalli 620 015, India
[b] University of Cluj, Faculty of Mathematics, R-3400 Cluj, CP 253, Romania

Received 12 May 2005; received in revised form 27 December 2005
Available online 22 March 2006

Abstract

This paper reports a theoretical investigation of the boundary layer flow over a vertical flat plate embedded in a porous medium filled with water near the vicinity of its density maximum associated with the temperature of 3.98 °C at atmospheric pressure. The study aims at determining similarity solutions of the governing boundary layer equations for a class of problems where the variable wall temperature (VWT), variable heat flux (VHF), or variable heat transfer coefficient (VHTC), vary as power functions of the distance from the leading edge of the plate. The existence and uniqueness of the solutions are considered and studied. The analytical and numerical solutions of the similarity form of the boundary layer equations yield velocity and temperature profiles as well as values of the stream function at the edge of the boundary layer, the heat transfer coefficient and the temperature on the plate.

Keywords: Porous medium; Non-Boussinesq fluid; Boundary layer

1. Introduction

Fluid flow and heat transfer in porous media have been of considerable interest, especially in the last several decades. This is primarily because of the numerous applications of flow through porous media, such as storage of radioactive nuclear waste materials, transpiration cooling, separation processes in chemical industries, filtration, transport processes in aquifers, groundwater pollution, etc. Theories and experiments of thermal convection in porous media, and the state-of-the-art reviews, with special emphasize on practical applications have been presented in the recent books by Nield and Bejan [1], Ingham and Pop [2], Vafai [3], Pop and Ingham [4], Bejan and Kraus [5], Ingham et al. [6] and Bejan et al. [7]. However, all the above mentioned studies are mainly restricted only to fluids at normal temperatures for which the Boussinesq approximation is valid and are not applied to fluids at the temperature of maximum density. Fluid density usually changes as a function of temperature in a reasonably linear manner. A notable exception is liquid water. Pure water at a pressure of one atmosphere has a maximum density of 999.9720 kg m^{-3} at 4 °C [8]. Above this temperature the density of water decreases as the temperature is increased in a manner similar to other fluids. For temperatures below 4 °C, however, the trend is reversed: density increases with increased temperature, giving rise to a maximum density at 4 °C point. Water and several metals have their maximum density in the liquid phase, ρ_c, at a temperature $T_c = 3.98$ °C above the melting temperature. Goren [9] has shown that for temperature sufficiently close to T_c, the relationship between fluid temperature, $\overline{T}$, and density, ρ, is given by the relation

$$\frac{\rho - \rho_c}{\rho_c} = -\gamma(\overline{T} - T_c)^2 \tag{1}$$

where ρ_c is the maximum density in the liquid phase and $\gamma = 8.0 \times 10^{-6}$ (°C)$^{-2}$ is the fluid thermal expansion coefficient of water at 4 °C. Moore and Weiss [10] state that (1)

* Corresponding author. Tel.: +91 9444808236; fax: +91 431 2500133.
E-mail address: sugunakumaran@yahoo.com (V. Kumaran).

0017-9310/$ - see front matter © 2006 Elsevier Ltd. All rights reserved.
doi:10.1016/j.ijheatmasstransfer.2006.01.026

Nomenclature

A_1, A_2	constants
g	gravitational acceleration, m/s^2
h	heat transfer coefficient for (VHTC), W/m^2
$\widetilde{K}$	permeability of the porous medium, m^2
l	streamwise length, m
L	length scale, m
m, n, r	constant exponents
q	heat flux for (VHF) case, W/m^2
$\overline{T}$	fluid temperature, K
T	dimensionless temperature
T_c	temperature at 3.98 °C
T_∞	ambient temperature, K
$\bar{u}, \bar{v}$	velocity components along $\bar{x}$- and $\bar{y}$-axes, respectively, m/s
U_c	characteristic velocity, m/s
$\bar{x}$, $\bar{y}$	Cartesian coordinates, m

Greek symbols

α	effective thermal diffusivity, m^2/s
γ	coefficient of thermal expansion, (°C)$^{-2}$
ε	small constant
θ	dimensionless temperature
ρ_c	maximum fluid density, kg/m^3
ν	kinematic viscosity, m^2/s
ψ	dimensionless stream function

is accurate to within ±4% in the range $0\ ^\circ\mathrm{C} \leqslant \overline{T} \leqslant 8\ ^\circ\mathrm{C}$. Gebhart and Mollendorf [11] give a relation, which is more accurate than (1) over a wider range of temperatures, but we shall follow here the many authors who have used (1). Thus, for small temperature variations free convection in water at T_c would be much reduced from that at other temperatures and this fact might be an important consideration in view of several physical problems, such as coolant in many experiments in chemical engineering, atomic energy, etc., where one wishes to suppress free convection.

The aim of this paper is, therefore, to study the steady free convection boundary layer flow over a vertical impermeable surface embedded in a porous medium saturated with water at 4 °C when the temperature of the plate, the surface heat flux, or, the heat transfer coefficient vary as a power function of the distance x from the leading edge of the plate. A generalized version of Newton's law of cooling (the rate of heat transfer at the wall is proportional to the excess temperature of the local fluid to that of the surrounding fluid, where the constant of proportionality is assumed to be varying with power of the coordinate along the plate) is also considered as a boundary condition and it is referred to as the prescribed heat transfer coefficient case for Boussinesq fluid by Ramanaiah and Malarvizhi [12], Ramanaiah and Kumaran [13,14]. Similar boundary condition is also considered for Boussinesq fluid by Merkin [15], Lesnic et al. [16] with a slight change in the condition (the rate of heat transfer at the wall is proportional to the temperature of the local fluid), which they referred it to as 'Newtonian heating'. Though many of these boundary conditions may be difficult to realize practically, all the above three classes of boundary conditions are chosen in the present study for the reason that these boundary conditions permit similarity solutions. The non-similar flows, like the case of Newtonian heating will be studied later. It should be mentioned that the problem of free convection in a porous cavity filled with water at 4 °C has been studied by Poulikakos [17,18], and Blake et al. [19].

2. Basic equations

Consider the steady free convection over a semi-infinite vertical impermeable flat plate which is embedded in a porous medium filled with water at 4 °C and maintained at a variable temperature (VWT), variable heat flux (VHF), or variable heat transfer coefficient (VHTC), and the ambient temperature being $T_\infty = T_c$. It is assumed that the convective fluid and the porous medium are in local thermodynamic equilibrium, the viscous dissipation is neglected, the physical properties of the fluid except the density are constant and that the Boussinesq and boundary layer approximations are valid. Under these assumptions, the governing equations are

$$\frac{\partial \bar{u}}{\partial \bar{x}} + \frac{\partial \bar{v}}{\partial \bar{y}} = 0 \tag{2}$$

$$\bar{u} = \frac{\widetilde{K} g \gamma}{\nu} (\overline{T} - T_c)^2 \tag{3}$$

$$\bar{u}\frac{\partial \overline{T}}{\partial \bar{x}} + \bar{v}\frac{\partial \overline{T}}{\partial \bar{y}} = \alpha \frac{\partial^2 \overline{T}}{\partial \bar{y}^2} \tag{4}$$

subjected to the boundary conditions

$$\bar{v} = 0 \quad \text{at } \bar{y} = 0 \tag{5a}$$

$$\bar{u} = 0, \quad \overline{T} = T_c \quad \text{as } \bar{y} \to \infty \tag{5b}$$

$$\text{(i) (VWT)} \quad \frac{\overline{T} - T_c}{T_c} = \left(\frac{\bar{x}}{l}\right)^m$$

$$\text{(ii) (VHF)} \quad -\frac{L}{T_c}\frac{\partial \overline{T}}{\partial \bar{y}} = \left(\frac{\bar{x}}{l}\right)^{(4m-1)/2} \qquad \text{at } \bar{y} = 0$$

$$\text{(iii) (VHTC)} \quad \frac{-L}{(\overline{T} - T_c)}\frac{\partial \overline{T}}{\partial \bar{y}} = \left(\frac{\bar{x}}{l}\right)^{(2m-1)/2} \tag{5c}$$

where $\bar{x}$ and $\bar{y}$ are the Cartesian coordinates along the plate and normal to it, $\bar{u}$ and $\bar{v}$ are velocity components along $\bar{x}$- and $\bar{y}$- axes, respectively, $\overline{T}$ is the fluid temperature, g is the acceleration due to gravity, $\widetilde{K}$ is the permeability of the

porous medium and α is the effective thermal diffusivity. Further, $L = \sqrt{l\alpha\nu/g\widetilde{K}\gamma T_c^2}$ is a length scale, m is a given constant, l is a given streamwise length scale and ν is the kinematic viscosity.

We now introduce the following dimensionless variables:

$$x = \bar{x}/l, \quad y = \bar{y}/L, \quad u = \bar{u}/U_c,$$
$$v = (l\bar{v})/(LU_c), \quad T = (\overline{T} - T_c)/T_c \tag{6}$$

where U_c is the characteristic velocity which is defined by: $U_c = (l\alpha)/L^2$. Eqs. (2)–(5) can then be written in non-dimensional form as, see Pop and Ingham [4],

$$\frac{\partial u}{\partial x} + \frac{\partial v}{\partial y} = 0 \tag{7}$$

$$u = T^2 \tag{8}$$

$$u\frac{\partial T}{\partial x} + v\frac{\partial T}{\partial y} = \frac{\partial^2 T}{\partial y^2} \tag{9}$$

subjected to the boundary conditions

$$v = 0 \quad \text{at } y = 0 \tag{10a}$$

$$u = 0, \quad T = 0 \quad \text{as } y \to \infty \tag{10b}$$

$$\text{(i) (VWT)} \quad T = T_{w0}(x) = x^m \quad \text{at } y = 0 \tag{10c}$$

$$\text{(ii) (VHF)} \quad -\left(\frac{\partial T}{\partial y}\right)_{y=0} = q_{w1}(x) = x^{(4m-1)/2} \tag{10d}$$

$$\text{(iii) (VHTC)} \quad -\left(\frac{1}{T}\frac{\partial T}{\partial y}\right)_{y=0} = h_{w2}(x) = x^{(2m-1)/2} \tag{10e}$$

3. Similarity solutions

(i) *Case of VWT*

In this case we assume the dimensionless wall temperature as

$$T_{w0}(x) = x^m \tag{11}$$

and introduce the following similarity variables:

$$\psi_0 = x^{(1+2m)/2} f_0(\eta_0), \quad T = x^m \theta_0(\eta_0), \quad \eta_0 = x^{(2m-1)/2} y \tag{12}$$

except $m = -1/2$ which has been treated separately in Appendix A. In (12) ψ_0 is the dimensionless stream function, which is defined in the usual way as $u = \partial\psi_0/\partial y$ and $v = -\partial\psi_0/\partial x$. Substituting variables (11) and (12) into Eqs. (8)–(10c), we get

$$f_0' = \theta_0^2 \tag{13}$$

$$\theta_0'' + \frac{1+2m}{2} f_0\theta_0' - m f_0'\theta_0 = 0 \tag{14}$$

subject to the boundary conditions

$$f_0(0) = 0, \quad \theta_0(0) = 1, \quad \theta_0(\infty) = 0 \tag{15}$$

Eq. 15(a) need not be ensured when $m = -1/2$, which has been treated separately in Appendix A. The quantity of interest is the heat transfer from the plate, which can be written in non-dimensional form as

$$q_{w0}(x) = x^{(4m-1)/2}[-\theta_0'(0)] \tag{16}$$

We notice that integrating Eq. (14) with the boundary conditions (15), we get the relation

$$\theta_0'(0) = -\frac{(1+4m)}{2}\int_0^\infty f_0'\theta_0 \, d\eta_0 \tag{17}$$

which shows that the plate is adiabatic for $m = -1/4$.

3.1. Numerical solutions for VWT case

Solving Eqs. (13)–(15) numerically for a range of values $-0.25 \leqslant m \leqslant 5000$, we obtain values of $-\theta_0'(0), f_0(\eta_{0\infty})$ and $\eta_{0\delta}$, respectively. The shooting method has been used to solve these equations. Some of these values are given in Table 1(a) where $\eta_{0\infty}$ is the value of η_0 at the free stream, given by $\theta_0(\eta_{0\infty}) = 10^{-10}$. It is seen that at $x = 1$, the dimensionless wall heat flux $-\theta_0'(0)$ increases with m, while the stream function value at the free stream $f_0(\eta_{0\infty})$ and the thermal boundary layer thickness $\eta_{0\delta}$ defined as $\theta_0(\eta_{0\delta}) = 0.01$ decreases with increasing m. It is also observed from the values of $\eta_{0\infty}$ that θ_0 approaches zero very fast when m approaches larger values. From Eq. (13), it is clear that f' will be always non-negative even in the down stream. Therefore it may be concluded that there are no multiple solutions in this range of m values. Note that in the Boussinesq fluid case, Ingham and Brown [20] reported multiple solutions due to the flow reversal in the down stream.

(ii) *Case of VHF*

Now, we assume the dimensionless wall heat flux as

$$q_{w1}(x) = x^n \tag{18}$$

where $n = (4m-1)/2$ and introduce the following similarity variables:

$$\psi_1 = x^{(1+2m)/2} f_1(\eta_1), \quad T = x^m \theta_1(\eta_1), \quad \eta_1 = x^{(2m-1)/2} y \tag{19}$$

Table 1(a)
Variation of $-\theta_0'(0), f_0(\eta_{0\infty}), \eta_{0\infty}$ and $\eta_{0\delta}$ with m for VWT case

m	$-\theta_0'(0)$	$f_0(\eta_{0\infty})$	$\eta_{0\infty}$	$\eta_{0\delta}$
−0.25	0.000001	1.999991	27.0	10.597
0	0.376526	1.090319	26.0	8.769
0.25	0.565140	0.838747	21.0	7.408
0.50	0.707107	0.707106	20.0	6.513
0.75	0.825530	0.622822	18.0	5.876
1	0.929182	0.562936	15.0	5.393
1.2	1.004503	0.525762	14.0	5.082
1.5	1.107990	0.481655	13.0	4.702
2	1.261829	0.427759	12.0	4.222
5	1.944541	0.284077	8.0	2.870
10	2.725929	0.204402	6.0	2.084
20	3.837976	0.145833	4.0	1.494
50	6.052145	0.092737	3.0	0.953
100	8.551380	0.065695	1.8	0.676
200	12.088118	0.046495	1.1	0.479
500	19.107853	0.029422	0.7	0.303
1000	27.020148	0.020808	0.5	0.215
2000	38.211272	0.014713	0.3	0.152
5000	60.415173	0.009307	0.2	0.096

where ψ_1 is the dimensionless stream function, which is defined in the usual way $u = \partial\psi_1/\partial y$ and $v = -\partial\psi_1/\partial x$. Substituting variables (18) and (19) into Eqs. (8)–(10b) and (10d), we get

$$f_1' = \theta_1^2 \tag{20}$$

$$\theta_1'' + \frac{1+2m}{2} f_1\theta_1' - m f_1'\theta_1 = 0 \tag{21}$$

subject to the boundary conditions

$$f_1(0) = 0, \quad \theta_1'(0) = -1, \quad \theta_1(\infty) = 0 \tag{22}$$

The quantity of interest is now the wall temperature, which is given in non-dimensional form by

$$T_{w1}(x) = x^{(2n+1)/4}\theta_1(0) \tag{23}$$

We have also the relation

$$(1+4m)\int_0^\infty f_1'\theta_1 \, d\eta_1 = 2 \tag{24}$$

The above relation shows that the solution of Eqs. (20)–(22) is possible only for $m > -1/4$, i.e., $n > -1$. Using the transformation

$$\eta_1 = \eta_0 A_1, \quad f_1(\eta_1) = f_0(\eta_0)/A_1, \quad \theta_1(\eta_1) = \theta_0(\eta_0)/A_1 \tag{25}$$

where A_1 is a positive constant which depends on the value of n alone, the boundary condition $\theta_1'(0) = -1$ gives

$$A_1 = (-\theta_0'(0))^{1/2} \tag{26}$$

Therefore, the dimensionless wall temperature at $x = 1$, takes the form

$$\theta_1(0) = (-\theta_0'(0))^{-1/2} \tag{27}$$

3.2. Numerical solutions for VHF case

Using the transformations (25) and (26), Eqs. (20)–(22) governing the case of wall heat flux varying as x^n, are solved numerically for some values of n in the range $-1 < n \leqslant 9999.5$. Values of $\theta_1(0)$, $f_1(\eta_{1\infty})$, $\eta_{1\infty}$ and A_1 are given in Table 1(b). It is observed that at $x = 1$, the values of the dimensionless wall temperature $\theta_1(0)$ and the stream function at the free stream $f_1(\eta_{1\infty})$ decreases with increasing n.

(iii) *Case of VHTC*

Now, we assume the dimensionless heat transfer coefficient as

$$h_{w2}(x) = x^r \tag{28}$$

where $r = (2m-1)/2$ and introduce the following similarity variables:

$$\psi_2 = x^{(1+2m)/2} f_2(\eta_2), \quad T = x^m\theta_2(\eta_2), \quad \eta_2 = x^{(2m-1)/2} y \tag{29}$$

where ψ_2 is the dimensionless stream function, which is defined in the usual way $u = \partial\psi_2/\partial y$ and $v = -\partial\psi_2/\partial x$.

Table 1(b)
Variation of $\theta_1(0)$, $f_1(\eta_{1\infty})$, $\eta_{1\infty}$ and A_1 with n for VHF case

n	$\theta_1(0)$	$f_1(\eta_{1\infty})$	$\eta_{1\infty}$	A_1
−1	∞	∞	∞	0
−0.5	1.629680	1.776871	15.9541	0.613617
0	1.330215	1.115714	15.7869	0.751758
0.5	1.189207	0.840896	16.8179	0.840897
1	1.100610	0.685484	16.3546	0.908587
1.5	1.037408	0.583994	14.4591	0.963941
1.9	0.997756	0.524582	14.0315	1.002249
2.5	0.950019	0.457581	13.6839	1.052611
3.5	0.890225	0.380802	13.4797	1.123311
9.5	0.717119	0.203717	11.1557	1.394468
19.5	0.605679	0.123802	9.9062	1.651039
39.5	0.510445	0.074440	7.8363	1.959075
99.5	0.406486	0.037696	7.3803	2.460111
199.5	0.341965	0.022465	5.2637	2.924274
399.5	0.287621	0.013373	3.8245	3.476797
999.5	0.228767	0.006731	3.0599	4.371253
1999.5	0.192378	0.004003	2.5990	5.198091
3999.5	0.161772	0.002380	1.8545	6.181527
9999.5	0.128655	0.001197	1.5545	7.772720

Substituting variables (28) and (29) into Eqs. (8)–(10b), and the boundary condition (10e), we get

$$f_2' = \theta_2^2 \tag{30}$$

$$\theta_2'' + \frac{1+2m}{2} f_2\theta_2' - m f_2'\theta_2 = 0 \tag{31}$$

subject to the boundary conditions

$$f_2(0) = 0, \quad \theta_2'(0) + \theta_2(0) = 0, \quad \theta_2(\infty) = 0 \tag{32}$$

The quantity of interest is again the wall temperature, which is given in non-dimensional form by

$$T_{w2}(x) = x^{(2r+1)/2}\theta_2(0) \tag{33}$$

Using the transformation

$$\eta_2 = \eta_0 A_2, \quad f_2(\eta_2) = f_0(\eta_0)/A_2, \quad \theta_2(\eta_2) = \theta_0(\eta_0)/A_2 \tag{34}$$

where A_2 is a positive constant which depends on the power r alone, relation $\theta_2'(0) + \theta_2(0) = 0$ gives

$$A_2 = -\theta_0'(0) \tag{35}$$

Therefore the dimensionless wall temperature at $x = 1$, is given by

$$\theta_2(0) = (-\theta_0'(0))^{-1} \tag{36}$$

3.3. Numerical solutions for VHTC case

Using the transformations (34) and (35), Eqs. (30)–(32) governing the case of wall heat transfer coefficient varying as x^r are solved numerically for a range values of r in the range $-0.75 < r \leqslant 4999.5$. Values of $\theta_2(0)$, $f_2(\eta_{2\infty})$, $\eta_{2\infty}$ and A_2 are given in Table 1(c). It is seen that at $x = 1$, the dimensionless wall temperature $\theta_2(0)$ and the stream function at the free stream $f_2(\eta_{2\infty})$, decreases with increasing r.

Table 1(c)
Variation of $\theta_2(0)$, $f_2(\eta_{2\infty})$, $\eta_{2\infty}$ and A_2 with r for VHTC case

r	$\theta_2(0)$	$f_2(\eta_{2\infty})$	$\eta_{2\infty}$	A_2
−0.75	∞	∞	∞	0
−0.5	2.655856	2.895730	9.7897	0.376526
−0.25	1.769472	1.484140	11.8679	0.565140
0	1.414213	0.999999	14.1421	0.707107
0.25	1.211343	0.754451	14.8595	0.825530
0.5	1.076216	0.605840	13.9377	0.929182
0.7	0.995517	0.523405	14.0630	1.004503
1	0.902536	0.434711	14.4039	1.107990
1.5	0.792501	0.338999	15.1419	1.261829
4.5	0.514260	0.146089	15.5563	1.944541
9.5	0.366847	0.074985	16.3556	2.725929
19.5	0.260554	0.037997	15.3519	3.837976
49.5	0.165231	0.015323	18.1564	6.052145
99.5	0.116940	0.007682	15.3925	8.551380
199.5	0.082726	0.003846	13.2969	12.088118
499.5	0.052335	0.001540	13.3755	19.107853
999.5	0.037009	0.000770	13.5101	27.020148
1999.5	0.026170	0.000385	11.4634	38.211272
4999.5	0.016552	0.000154	12.0830	60.415173

3.4. Some analytical solutions

It is worth mentioning that for the case of VWT there are exact analytical solutions of Eqs. (13)–(15) for some values of m and they are given by

$$f_0(\eta_0) = \frac{1}{\sqrt{2}}\left(1 - e^{-\eta_0\sqrt{2}}\right), \quad \theta_0(\eta_0) = e^{-\eta_0/\sqrt{2}} \tag{37}$$

when $m = 1/2$ and

$$f_0(\eta_0) = 2\tanh\left(\frac{\eta_0}{2}\right), \quad \theta_0(\eta_0) = \operatorname{sech}\left(\frac{\eta_0}{2}\right) \tag{38}$$

when $m = -1/4$.

Corresponding to the solution of $m = 1/2$ (VWT case), using the transformations (25) and (26), we get one exact analytical solution of Eqs. (20)–(22) for the case of VHF, given by

$$f_1(\eta_1) = \frac{1}{2^{1/4}}(1 - e^{-\eta_1 2^{3/4}}), \quad \theta_1(\eta_1) = 2^{1/4}e^{-\eta_1/2^{1/4}} \tag{39}$$

when $n = 1/2$. Also, using (34) and (35), we get one exact analytical solution of Eqs. (30)–(32) for the case VHTC, given by

$$f_2(\eta_2) = 1 - e^{-2\eta_2}, \quad \theta_2(\eta_2) = \sqrt{2}e^{-\eta_2} \tag{40}$$

when $r = 0$.

3.5. Non-existence of solutions for $m \leqslant -\frac{1}{3}$, $n \leqslant -1$ and $r \leqslant -\frac{3}{4}$

From (13) and (15a) it results in that $f_0' \geqslant 0$ and $f_0 \geqslant 0$ for all $m \neq -1/2$. Multiplying Eq. (14) by f_0 and integrating using the boundary conditions (15), we get

$$\int_0^{f_0(\infty)} f_0\theta_0\,\mathrm{d}f_0 = \frac{1}{3(3m+1)} \tag{41}$$

Thus the above integral becomes negative for $m < -1/3$ and infinity for $m = -1/3$, respectively. Hence we conclude that there is no solution for VWT case when $m \leqslant -1/3$. We notice from Table 1(a), $\theta_0'(0)$ is negative only for $m > -0.25$. Using this fact it is clear from (26) and (35), that A_1 and A_2 are positive only for $n > -1$ and $r > -3/4$, respectively. Hence, it may be concluded that there is no solution for the range $n \leqslant -1$ for VHF case and also there is no solution for the range $r \leqslant -3/4$ for VHTC case. Note that the same conclusion for VHF case has been obtained already in Eq. (24).

3.6. Asymptotic solutions for m close to $-1/3$

Let us take

$$m = -\frac{1}{3} + \varepsilon \tag{42}$$

where $\varepsilon > 0$ is a small positive constant. Using the transformations

$$f_0(\eta_0) = \varepsilon^{-s}F(\xi), \quad \theta_0(\eta_0) = \varepsilon^{-s}H(\xi), \quad \eta_0 = \varepsilon^s\xi \tag{43}$$

in (41) gives $s = 1/3$ and $\int_0^\infty F(\xi)H(\xi)H'(\xi)\,\mathrm{d}\xi = 1/9$. Eqs. (13)–(15) then become

$$F' = H^2 \tag{44}$$

$$H'' + \left(\frac{1}{6} + \varepsilon\right)FH' + \left(\frac{1}{3} - \varepsilon\right)F'H = 0 \tag{45}$$

subject to the boundary conditions

$$F(0) = 0, \quad H(0) = \varepsilon^{1/3}, \quad H(\infty) = 0 \tag{46}$$

Assuming

$$f_0(\eta_0, \varepsilon) = \varepsilon^{-1/3}F(\xi, \varepsilon) = \varepsilon^{-1/3}F_0(\xi) + F_1(\xi) + \cdots \tag{47}$$

$$\theta_0(\eta_0, \varepsilon) = \varepsilon^{-1/3}H(\xi, \varepsilon) = \varepsilon^{-1/3}H_0(\xi) + H_1(\xi) + \cdots \tag{48}$$

in Eqs. (44)–(46), we get

$$F_0' = H_0^2 \tag{49}$$

$$H_0'' + \frac{1}{6}F_0H_0' + \frac{1}{3}F_0'H_0 = 0 \tag{50}$$

subject to the boundary conditions

$$F_0(0) = 0, \quad H_0(0) = 0, \quad H_0(\infty) = 0 \tag{51}$$

and so on.

An investigation of Eq. (50), shows that if it is multiplied by F_0, then one integration can be performed and, on using (49) and (51), we get

$$F_0H_0' - \frac{1}{3}H_0^3 + \frac{1}{6}F_0^2H_0 = 0 \tag{52}$$

Let $P_0(F_0) = F_0'$, and integrating (52), we obtain

$$P_0 = F_0' = \frac{1}{4}(A^{4/3}F_0^{2/3} - F_0^2) \tag{53}$$

where $F_0 \to A$ as $\xi \to \infty$. Hence, we have

$$H_0'(0) = \frac{A^2}{24} \tag{54}$$

The unknown constant A may be determined from the condition (41). Using Eqs. (52)–(54), the condition (41) may be rewritten as

$$\int_0^A F_0^{4/3}\sqrt{A^{4/3}-F_0^{4/3}}\,\mathrm{d}F_0=\frac{2}{9} \tag{55}$$

The substitution $F_0=A\sin^{3/2}\theta$, converts the integral in (55) as follows:

$$\frac{8}{27A^3}=2\int_0^{\pi/2}(\sin^{5/2}\theta)(\cos^2\theta)\,\mathrm{d}\theta=\beta\left(\frac{7}{4},\frac{3}{2}\right) \tag{56}$$

where the last term is the beta integral. Using the Gamma integral tables, we obtain

$$F_0(\infty)=A=0.975176615\ldots \tag{57}$$

Therefore

$$H_0'(0)=\frac{A^2}{24}=0.039623726\ldots \tag{58}$$

Solving equations corresponding to F_1 and H_1, it was found that it has no effect on neither $\theta_0'(0)$ nor $f_0(\infty)$. Therefore, we have

$$\theta_0'(0)\approx\frac{A^2}{24}\varepsilon^{-2/3},\quad f_0(\infty)\approx A\varepsilon^{-1/3} \tag{59}$$

when $m=-\frac{1}{3}+\varepsilon$ and $\varepsilon>0$ for VWT case.

The results given by (59) are compared with exact numerical solution of Eqs. (13)–(15), in Table 2. Good agreement between the values are seen when $m\to-\frac{1}{3}$.

3.7. Series solutions for $m=-\frac{1}{4}+\varepsilon$, $n=-1+2\varepsilon$ and $r=-\frac{3}{4}+\varepsilon$

Since for $m=-1/4$ the plate is adiabatic, i.e., $\theta_0'(0)=0$, it is worth to get a series solution valid near $m=-1/4$. Let $m=-\frac{1}{4}+\varepsilon$, where ε is a small constant and assume the series

$$f_0=F_0+\varepsilon F_1+\varepsilon^2F_2+\cdots,$$
$$\theta_0=H_0+\varepsilon H_1+\varepsilon^2H_2+\cdots \tag{60}$$

Table 2
Variation of $\theta_0'(0)$ and $f_0(\infty)$ with $m=-\frac{1}{3}+\varepsilon$ and asymptotic approach to $\varepsilon\to0$ (i.e., $m\to-\frac{1}{3}$) for VWT case

ε	$\theta_0'(0)$	$\frac{A^2}{24}\varepsilon^{-2/3}$	$f_0(\infty)$	$A\varepsilon^{-1/3}$
0.00001	85.422176	85.366750	45.277758	45.263694
0.00002	53.793865	53.777682	35.930279	35.925818
0.00005	29.196298	29.195017	26.469383	26.470368
0.0001	18.389201	18.391708	21.005898	21.009545
0.0002	11.580994	11.586050	16.668680	16.675287
0.0005	6.280811	6.289875	12.273911	12.286456
0.001	3.948666	3.962373	9.731884	9.751767
0.002	2.475320	2.496139	7.708753	7.739982
0.005	1.318549	1.355113	5.647109	5.702868
0.01	0.797350	0.853667	4.441794	4.526369
0.03	0.298716	0.410400	2.985880	3.138409
0.05	0.139175	0.291950	2.455134	2.647037

in Eqs. (13)–(15). We then get

$$F_0'=H_0^2 \tag{61}$$
$$H_0''+\frac{1}{4}(F_0H_0'+F_0'H_0)=0 \tag{62}$$
$$F_1'=2H_0H_1 \tag{63}$$
$$H_1''+\frac{1}{4}(F_1H_0'+F_0H_1'+F_0'H_1+F_1'H_0)+F_0H_0'-F_0'H_0=0 \tag{64}$$
$$F_2'=2H_0H_2+H_1^2 \tag{65}$$
$$H_2''+\frac{1}{4}(F_2H_0'+F_1H_1'+F_0H_2'+F_2'H_0+F_1'H_1+F_0'H_2)+F_1H_0'+F_0H_1'-F_1'H_0-F_0'H_1=0 \tag{66}$$

subject to the boundary conditions

$$\begin{aligned}&F_0(0)=0,\quad H_0(0)=1,\quad H_0(\infty)=0,\quad F_1(0)=0,\\&H_1(0)=0,\quad H_1(\infty)=0,\\&F_2(0)=0,\quad H_2(0)=0,\quad H_2(\infty)=0\end{aligned} \tag{67}$$

Note that Eqs. (61), (62) and (67a,b,c) are solved analytically for F_0 and H_0, and the solution is given in Eq. (38). Integrating Eq. (64) once from 0 to ∞ and using the boundary conditions (67), we get $H_1'(0)=-\pi$.

On the other hand, solving the set of coupled Eqs. (61)–(67), numerically, we get

$$\theta_0'(0)=-3.14159265\varepsilon+20.67085113\varepsilon^2+\cdots \tag{68a}$$
$$f_0(\infty)=2-9.8696044\varepsilon+77.8930842\varepsilon^2+\cdots \tag{68b}$$

when $m=-\frac{1}{4}+\varepsilon$ for VWT case.

Further, using (68) in the transformations (25) and (26), we get

$$A_1\approx\sqrt{\pi\varepsilon(1-6.5797363\varepsilon)},\quad \theta_1(0)\approx1/A_1 \tag{69a}$$
$$f_1(\infty)\approx(2-9.8696044\varepsilon+77.8930842\varepsilon^2)/A_1 \tag{69b}$$

when $n=-1+2\varepsilon$, $\varepsilon>0$ for VHF case. On using (68) in the transformations (34) and (35), we get

$$A_2\approx\pi\varepsilon(1-6.5797363\varepsilon),\quad \theta_2(0)\approx1/A_2 \tag{70a}$$
$$f_2(\infty)\approx(2-9.8696044\varepsilon+77.8930842\varepsilon^2)/A_2 \tag{70b}$$

when $r=-\frac{3}{4}+\varepsilon$, $\varepsilon>0$ for VHTC case.

The results given in Eqs. (68)–(70) are compared with the exact numerical solutions of Eqs. (13)–(15), (20)–(22) and (30)–(32) in Tables 3(a), 3(b) and 3(c), respectively. It is observed the results agree well when $m\to-0.25+$, $n\to-1+$ and $r\to-0.75+$ for VWT, VHF and VHTC cases, respectively. The convergence of the series solutions is slightly faster for $m>-0.25$ when compared to $m<-0.25$ for VWT case.

3.8. Series solutions for $m=0+\varepsilon$, $n=-\frac{1}{2}+2\varepsilon$ and $r=-\frac{1}{2}+\varepsilon$

For small m, let $m=\varepsilon$, where ε is a small constant and assuming the series

Table 3(a)
Comparison of series solutions near $m = -0.25$ (Eqs. (68)) with exact numerical solutions for VWT case

ε	$m = -\frac{1}{4} + \varepsilon$	$\theta_0'(0)$	Eq. (68a)	$f_0(\infty)$	Eq. (68b)
−0.05	−0.3	0.263374	0.208757	2.869732	2.688213
−0.01	−0.26	0.033706	0.033483	2.107275	2.106485
−0.005	−0.255	0.016251	0.016225	2.051389	2.051295
−0.001	−0.251	0.003162	0.003162	2.009948	2.009947
−0.0005	−0.2505	0.001576	0.001576	2.004954	2.004954
−0.0001	−0.2501	0.000314	0.000314	2.000988	2.000988
0	−0.25	0	0	2	2
0.0001	−0.2499	−0.000314	−0.000314	1.999014	1.999014
0.0005	−0.2495	−0.001566	−0.001566	1.995085	1.995085
0.001	−0.249	−0.003121	−0.003121	1.990208	1.990208
0.005	−0.245	−0.015215	−0.015191	1.952515	1.952599
0.01	−0.24	−0.029529	−0.029349	1.908445	1.909093
0.05	−0.2	−0.121795	−0.105403	1.641314	1.701252

Table 3(b)
Comparison of series solutions for $n = -1 + 2\varepsilon$ (Eqs. (69)) with exact numerical solutions for VHF case ($\varepsilon > 0$)

ε	$\theta_1(0)$	Eq. (69a)	$f_1(\infty)$	Eq. (69b)
0.0001	56.4375	56.4375	112.81936	112.81940
0.0005	25.2727	25.2729	50.42124	50.42164
0.001	17.8997	17.9002	35.62404	35.62518
0.005	8.1071	8.1134	15.82926	15.84226
0.01	5.8194	5.8372	11.10592	11.14376
0.05	2.8654	3.0802	4.70302	5.24015

Table 3(c)
Comparison of series solutions for $r = -\frac{3}{4} + \varepsilon$ (Eqs. (70)) with exact numerical solutions for VHTC case ($\varepsilon > 0$)

ε	$\theta_2(0)$	Eq. (70a)	$f_2(\infty)$	Eq. (70b)
0.0001	3185.192	3185.195	6367.244	6367.248
0.0005	638.711	638.721	1274.282	1274.303
0.001	320.398	320.418	637.658	637.699
0.005	65.725	65.828	128.330	128.535
0.01	33.865	34.073	64.629	65.048
0.05	8.211	9.487	13.476	16.141

$$f_0 = F_0 + \varepsilon F_1 + \varepsilon^2 F_2 + \cdots \tag{71}$$

$$\theta_0 = H_0 + \varepsilon H_1 + \varepsilon^2 H_2 + \cdots \tag{72}$$

in Eqs. (13)–(15), we get

$$F_0' = H_0^2 \tag{73}$$

$$H_0'' + \frac{1}{2} F_0 H_0' = 0 \tag{74}$$

$$F_1' = 2H_0 H_1 \tag{75}$$

$$H_1'' + \frac{1}{2}(F_1 H_0' + F_0 H_1') + F_0 H_0' - F_0' H_0 = 0 \tag{76}$$

$$F_2' = 2H_0 H_2 + H_1^2 \tag{77}$$

$$H_2'' + \frac{1}{2}(F_2 H_0' + F_1 H_1' + F_0 H_2') + F_1 H_0' + F_0 H_1' - F_1' H_0 - F_0' H_1 = 0 \tag{78}$$

subject to the boundary conditions

$$\begin{aligned} &F_0(0) = 0, \quad H_0(0) = 1, \quad H_0(\infty) = 0 \\ &F_1(0) = 0, \quad H_1(0) = 0, \quad H_1(\infty) = 0 \\ &F_2(0) = 0, \quad H_2(0) = 0, \quad H_2(\infty) = 0 \end{aligned} \tag{79}$$

Solving the above set of coupled Eqs. (73)–(79), numerically we get,

$$\theta_0'(0) = -0.376526 - 0.922721\varepsilon + 0.982136\varepsilon^2 + \cdots \tag{80a}$$

$$f_0(\infty) = 1.090320 - 1.509365\varepsilon + 3.167386\varepsilon^2 + \cdots \tag{80b}$$

for VWT case when $m = \varepsilon$.

Further, using (80) in the transformations (25) and (26), we get

$$A_1 \approx \sqrt{0.376526 + 0.922721\varepsilon - 0.982136\varepsilon^2}$$

$$\theta_1(0) \approx 1/A_1 \tag{81a}$$

$$f_1(\infty) \approx (1.090320 - 1.509365\varepsilon + 3.167386\varepsilon^2)/A_1 \tag{81b}$$

for VHF case when $n = -0.5 + 2\varepsilon$. Thus, using (80) in the transformations (34) and (35), we get

$$A_2 \approx 0.376526 + 0.922721\varepsilon - 0.982136\varepsilon^2$$

$$\theta_2(0) \approx 1/A_2 \tag{82a}$$

$$f_2(\infty) \approx (1.090320 - 1.509365\varepsilon + 3.167386\varepsilon^2)/A_2 \tag{82b}$$

for VHTC case when $r = -0.5 + \varepsilon$.

The results given in Eqs. (80)–(82) are compared with the exact numerical solutions of Eqs. (13)–(15), (20)–(22) and (30)–(32) in Tables 4(a), 4(b) and 4(c), respectively. It is observed the results agree well when $m \to 0$, $n \to -0.5$ and $r \to -0.5$ for VWT, VHF and VHTC cases, respectively. The convergence of the series solutions is faster for $m > 0$ when compared to $m < 0$ for VWT case.

3.9. Asymptotic solutions for large m, n and r

For large values of m, using the transformation,

$$f_0(\eta_0) = m^{-1/2} F_0(\xi_0), \quad \theta_0(\eta_0) = H_0(\xi_0), \quad \eta_0 = m^{-1/2}\xi_0 \tag{83}$$

Table 4(a)
Comparison of series solutions for $m = 0 + \varepsilon$ (Eqs. (80)) with exact numerical solutions for VWT case

ε	$\theta_0'(0)$	Eq. (80a)	$f_0(\infty)$	Eq. (80b)
−0.2	−0.121795	−0.152696	1.641313	1.518888
−0.1	−0.271883	−0.274433	1.282891	1.272930
−0.05	−0.327660	−0.327935	1.174771	1.173707
−0.005	−0.371888	−0.371888	1.097947	1.097946
−0.001	−0.375603	−0.375602	1.091832	1.091833
−0.0001	−0.376434	−0.376434	1.090471	1.090471
0	−0.376526	−0.376526	1.090320	1.090320
0.0001	−0.376618	−0.376618	1.090169	1.090169
0.001	−0.377448	−0.377448	1.088814	1.088814
0.005	−0.381116	−0.381115	1.082851	1.082852
0.05	−0.420424	−0.420207	1.021941	1.022770
0.1	−0.460551	−0.458977	0.965081	0.971057
0.2	−0.532428	−0.521785	0.875169	0.915142

Table 4(b)
Comparison of series solutions for $n = -0.5 + 2\varepsilon$ (Eqs. (81)) with exact numerical solutions for VHF case

ε	$\theta_1(0)$	Eq. (81a)	$f_1(\infty)$	Eq. (81b)
−0.2	2.865398	2.559091	4.703018	3.886973
−0.1	1.917825	1.908896	2.460362	2.429891
−0.05	1.746981	1.746250	2.052304	2.049585
−0.005	1.639812	1.639812	1.800427	1.800425
−0.001	1.631683	1.631683	1.781525	1.781525
−0.0001	1.629880	1.629880	1.777337	1.777337
0	1.629680	1.629681	1.776873	1.776873
0.0001	1.629481	1.629481	1.776409	1.776410
0.001	1.627689	1.627690	1.772250	1.772251
0.005	1.619838	1.619839	1.754044	1.754047
0.05	1.542256	1.542654	1.576095	1.577780
0.1	1.473538	1.476062	1.422084	1.433341
0.2	1.370470	1.384377	1.199393	1.266902

Table 4(c)
Comparison of series solutions for $r = -0.5 + \varepsilon$ (Eqs. (82)) with exact numerical solutions for VHTC case

ε	$\theta_2(0)$	Eq. (82a)	$f_2(\infty)$	Eq. (82b)
−0.2	8.210503	6.548945	13.476017	9.947116
−0.1	3.678054	3.643883	4.718544	4.638409
−0.05	3.051943	3.049388	3.585336	3.579088
−0.005	2.688983	2.688983	2.952361	2.952358
−0.001	2.662389	2.662391	2.906883	2.906885
−0.0001	2.656509	2.656510	2.896846	2.896847
0	2.655858	2.655859	2.895735	2.895736
0.0001	2.655207	2.655208	2.894625	2.894626
0.001	2.649372	2.649373	2.884673	2.884674
0.005	2.623877	2.623880	2.841269	2.841274
0.05	2.378552	2.379781	2.430741	2.433969
0.1	2.171315	2.178760	2.095495	2.115701
0.2	1.878187	1.916499	1.643732	1.753870

in the following approximated (for large m) form of Eqs. (13)–(15):

$$f_0' = \theta_0^2 \tag{84}$$

$$\theta_0'' + m f_0 \theta_0' - m f_0' \theta_0 = 0 \tag{85}$$

subject to the boundary conditions

$$f_0(0) = 0, \quad \theta_0(0) = 1, \quad \theta_0(\infty) = 0 \tag{86}$$

we get

$$F_0' = H_0^2 \tag{87}$$

$$H_0'' + F_0 H_0' - F_0' H_0 = 0 \tag{88}$$

subject to the boundary conditions

$$F_0(0) = 0, \quad H_0(0) = 1, \quad H_0(\infty) = 0 \tag{89}$$

Solving Eqs. (87)–(89), numerically we get

$$H_0'(0) = -0.854371, \quad F_0(\infty) = 0.658158 \tag{90}$$

Therefore,

$$\theta_0'(0) \approx -0.854371 m^{1/2}, \quad f_0(\infty) \approx 0.658158 m^{-1/2} \tag{91}$$

for VWT case when $m \gg 1$.

Using (91) in the transformations (25) and (26), we get

$$A_1 \approx 0.9243219 \left(\frac{n}{2} + \frac{1}{4}\right)^{1/4} \approx 0.777259 n^{1/4} \tag{92a}$$

$$f_1(\infty) \approx 1.197511 n^{-3/4}, \quad \theta_1(0) \approx 1.286572 n^{-1/4} \tag{92b}$$

for VHF case when $n \gg 1$. With the help of (91) and the transformation (34) and (35), we get

$$A_2 \approx 0.854371 \left(r + \frac{1}{2}\right)^{1/2} \approx 0.854371 r^{1/2} \tag{93a}$$

$$f_2(\infty) \approx 0.770342 r^{-1}, \quad \theta_2(0) \approx 1.170452 r^{-1/2} \tag{93b}$$

for VHTC case when $r \gg 1$.

On the other hand, the results given in Eqs. (91)–(93) are compared with exact numerical solutions of Eqs. (13)–(15), (20)–(22) and (30)–(32) in Tables 5(a), 5(b) and 5(c) respectively. Excellent agreement between the values are seen when $m \to \infty$, $n \to \infty$ and $r \to \infty$ for VWT, VHF and VHTC cases, respectively.

Table 5(a)
Variation of $-\theta_0'(0)$ and $f_0(\infty)$ with m and asymptotic approach to $m \to \infty$ for VWT case

m	$-\theta_0'(0)$	$0.854371 m^{1/2}$	$f_0(\infty)$	$0.658158 m^{-1/2}$
5	1.944541	1.9104	0.284077	0.2943
10	2.725929	2.7018	0.204402	0.2081
50	6.052145	6.0413	0.092737	0.0931
100	8.551380	8.5437	0.065695	0.0658
500	19.107853	19.1043	0.029422	0.029434
1000	27.020148	27.0176	0.020808	0.020813
5000	60.415173	60.4132	0.009307	0.009308

Table 5(b)
Variation of $\theta_1(0)$ and $f_1(\infty)$ with n and asymptotic approach to $n \to \infty$ for VHF case

n	$\theta_1(0)$	$1.286572 n^{-1/4}$	$f_1(\infty)$	$1.197511 n^{-3/4}$
9.5	0.717120	0.732830	0.203718	0.221302
19.5	0.605679	0.612245	0.123803	0.129048
99.5	0.406486	0.407360	0.037696	0.038012
199.5	0.341965	0.342333	0.022465	0.022560
999.5	0.228768	0.228817	0.006731	0.006736
1999.5	0.192379	0.192399	0.004003	0.004004
9999.5	0.128656	0.128659	0.001197	0.001198

Table 5(c)
Variation of $\theta_2(0)$ and $f_2(\infty)$ with r and asymptotic approach to $r \to \infty$ for VHTC case

r	$\theta_2(0)$	$1.170452 r^{-1/2}$	$f_2(\infty)$	$0.770342 r^{-1}$
4.5	0.514260	0.551756	0.146090	0.171187
9.5	0.366848	0.379745	0.074985	0.081089
49.5	0.165231	0.166361	0.015323	0.015562
99.5	0.116940	0.117339	0.007682	0.007742
499.5	0.052335	0.052370	0.001540	0.001542
999.5	0.037010	0.037022	0.000770	0.000771
4999.5	0.016552	0.016554	0.000154	0.000154

4. Results and discussion

Profiles of the dimensionless temperature θ_0 at $x = 1$ for VWT case for values of the range of values of m in the ranges $-1/3 < m < -0.25$ and $-0.25 \leqslant m \leqslant 100$ are shown in Figs. 1(a) and 1(b), respectively. For $-1/3 < m < -0.25$, the temperature close to the plate is greater when compared to that of the plate. The maximum temperature is attained very near to the plate (within the boundary layer) and the maximum move towards the plate when $m \to -1/3$. Also the temperature profiles have a very long and thin tail when $m \to -1/3$. On the other hand, for $-0.25 \leqslant m \leqslant 100$, the maximum temperature is at the plate itself.

Profiles of the dimensionless stream function f_0 at $x = 1$ for VWT case and for values of m in the ranges $-1/3 < m < -0.25$ and $-0.25 \leqslant m \leqslant 100$ are shown in

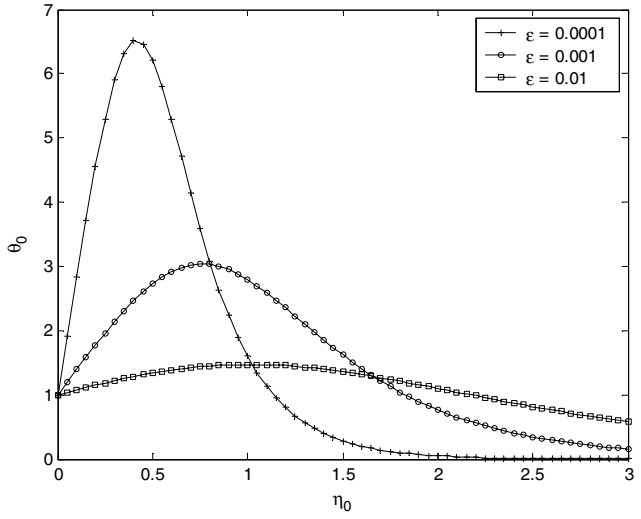

Fig. 1(a). Plots of θ_0 for values of $m = -\frac{1}{3} + \varepsilon,\ \varepsilon > 0$ (VWT case).

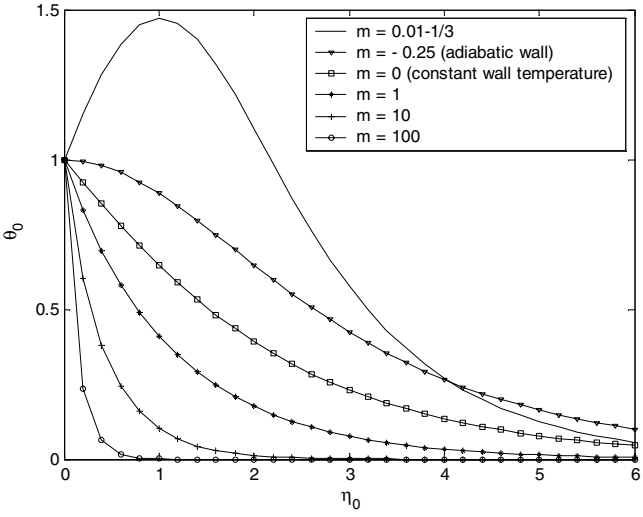

Fig. 1(b). Plots of θ_0 for various values of m (VWT case).

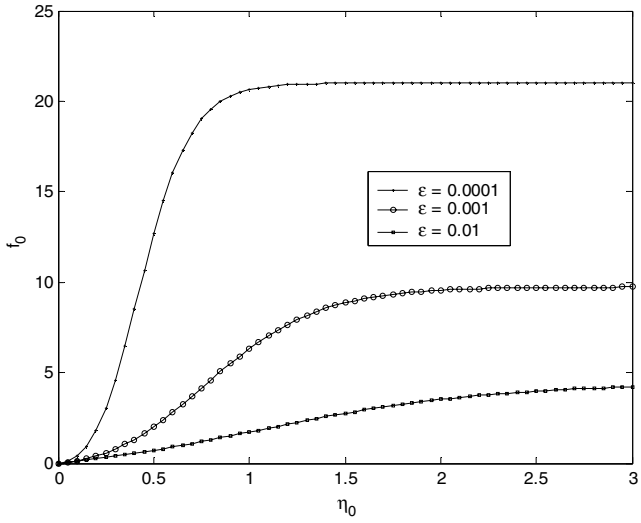

Fig. 2(a). Plots of f_0 for values of $m = -\frac{1}{3} + \varepsilon,\ \varepsilon > 0$ (VWT case).

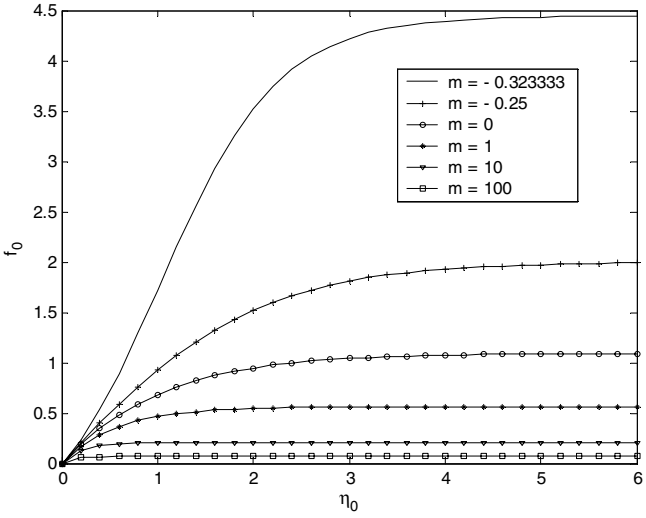

Fig. 2(b). Plots of f_0 for various values of m (VWT case).

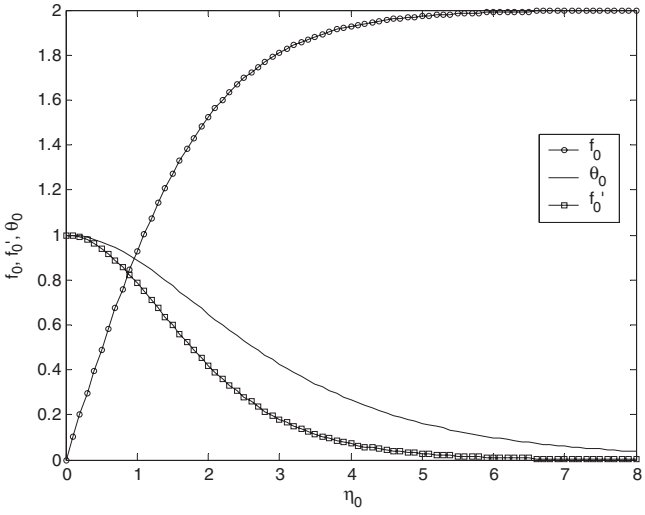

Fig. 3. Plots of f_0, f_0', θ_0 for adiabatic wall case (VWT case, $m = -0.25$).

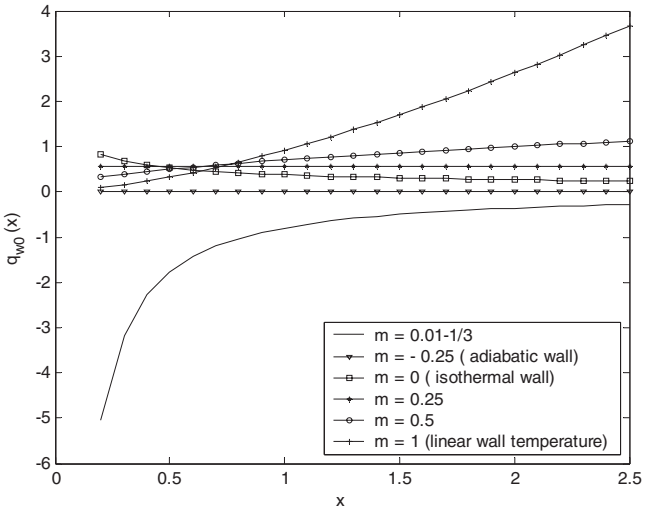

Fig. 4. Variation of dimensionless wall heat flux with x for various values of m (VWT case).

Figs. 2(a) and 2(b), respectively. For the range $-1/3 < m < -0.25$, the profiles of f_0 are concave near the plate, hence grows vertically steep and attains a larger constant value, whereas for the range $-0.25 \leqslant m \leqslant 100$, the profiles of f_0 are convex near the plate, hence grows gradually and attains a smaller constant value.

From Eq. (8), it is interesting to observe that since $u = T^2$, the momentum boundary layer thickness will be always less or equal when compared to the thermal boundary layer thickness. This is also seen from Fig. 3, where the plots of f_0 and of the dimensionless velocity profile f_0' as well as of θ_0 at $x = 1$, see Eq. (38) are shown for the adiabatic VWT case ($m = -0.25$).

Fig. 4 shows the variation of dimensionless wall heat flux $q_{w0}(x)$ with x for VWT case, Eq. (16). It is seen that q_{w0} is negative for $-1/3 < m < -0.25$, positive for $m > -0.25$ and zero for $m = -0.25$ (adiabatic wall case). When $m = 0.25$ and $m = -0.25$, q_{w0} is constant for all x, q_{w0} increases with increasing x for $-1/3 < m < -0.25$ and $m > 0.25$ whereas q_{w0} decreases with increasing x for $-0.25 < m < 0.25$. The results of Boussinesq fluid [20] and the non-Boussinesq fluid (present VWT case) are summarized in Table 6. It revealed a similar behaviour with m in both, except for a shift in the values of m.

In Figs. 5 and 6 an interesting comparison has been made between Boussinesq fluid [20] and non-Boussinesq

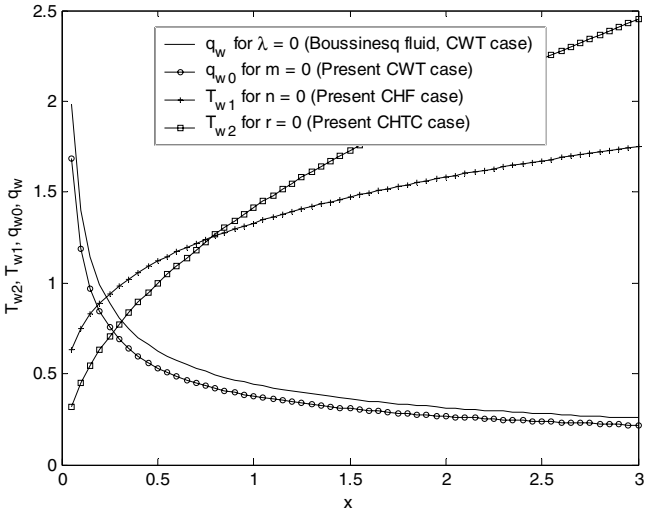

Fig. 5. Variation of the dimensionless wall heat flux with x for $\lambda = 0$ [20], $m = 0$ and variation of the dimensionless wall temperature with x for $n = 0$, $r = 0$.

Table 6
Comparison of results for Boussinesq fluid and Water at 4 °C for VWT case

Boussinesq fluid [20]	Non-Boussinesq fluid (present study for VWT case)
$T_w(x) = x^{\lambda}$	$T_{w0}(x) = x^{m}$
$q_w(x) = -x^{(3\lambda-1)/2}\theta'(0)$, $\psi(x,\infty) = x^{(\lambda+1)/2}f(\infty)$	$q_{w0}(x) = -x^{(4m-1)/2}\theta_0'(0)$, $\psi_0(x,\infty) = x^{(2m+1)/2}f_0(\infty)$
Analytical solutions for $\lambda = -\frac{1}{3}$ and $\lambda = 1$	Analytical solutions for $m = -\frac{1}{4}$ and $m = \frac{1}{2}$
Adiabatic solution for $\lambda = -\frac{1}{3}$	Adiabatic solution for $m = -\frac{1}{4}$
Multiple solutions for $\lambda > 1$	No multiple solutions
No solutions for $\lambda \leqslant -\frac{1}{2}$	No solutions for $m \leqslant -\frac{1}{3}$
Asymptotic solutions for $\lambda = -\frac{1}{2} + \varepsilon$ $\theta'(0) \approx 0.078103\varepsilon^{-3/4}$, $f(\infty) \approx 1.77828\varepsilon^{-1/4}$	Asymptotic solutions for $m = -\frac{1}{3} + \varepsilon$, $\varepsilon > 0$ $\theta_0'(0) \approx 0.039624\varepsilon^{-2/3}$, $f_0(\infty) \approx 0.975177\varepsilon^{-1/3}$
–	Series solutions for $m = -0.25 + \varepsilon$ $\theta_0'(0) = -3.14159265\varepsilon + 20.67085113\varepsilon^2 + \cdots$
Series solutions for $\lambda \to 0$ $\theta'(0) = -.44375 - .85665\lambda + .66943\lambda^2 + \cdots$	Series solutions for $m \to 0$ $\theta_0'(0) = -.376526 - .922721m + .982136m^2 + \cdots$
Asymptotic solutions for $\lambda \to \infty$ $\theta'(0) \approx -0.90638\lambda^{1/2}$, $f(\infty) \approx 1.28077\lambda^{-1/2}$	Asymptotic solutions for $m \to \infty$ $\theta_0'(0) \approx -0.854371m^{1/2}$, $f_0(\infty) \approx 0.658158m^{-1/2}$
Momentum boundary layer thickness is equal to thermal boundary layer thickness	Momentum boundary layer thickness is less than the thermal boundary layer thickness

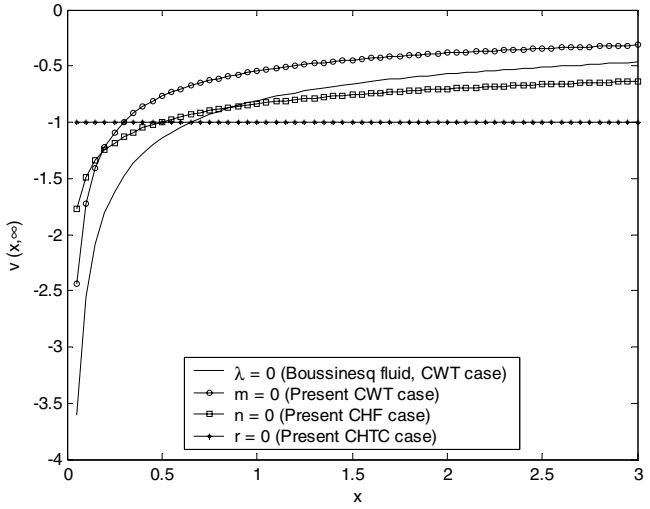

Fig. 6. Variation of $v(x,\infty)$ with x for $\lambda = 0$ [20], $m = 0$, $n = 0$ and $r = 0$.

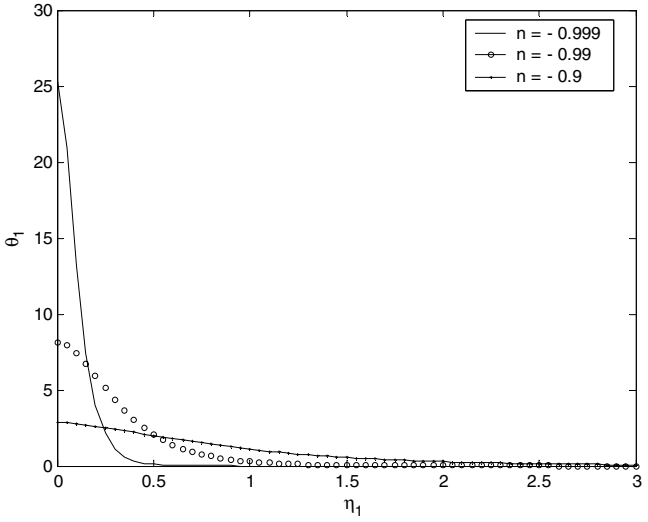

Fig. 7. Plots of θ_1 for values of n near -1 (VHF case).

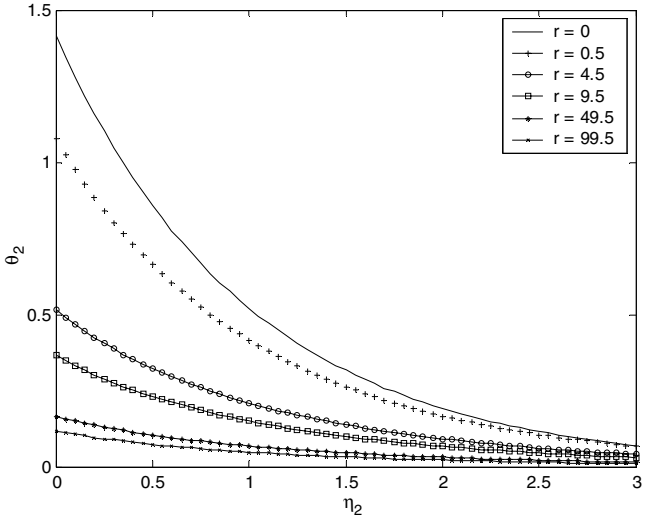

Fig. 8. Plots of θ_2 for various values of r (VHTC case).

fluid (present study) for constant wall temperature case. It is observed that the dimensionless wall heat flux and the dimensionless velocity component normal to the plate, towards the plate at the free stream ($-v(x,\infty)$) are smaller for non-Boussinesq fluid when compared to Boussinesq fluid for all x values.

The results for VHF and VHTC cases of the present study are summarized in Table 7. From the Figs. 7 and 8, it is seen that θ_1 and θ_2 (dimensionless temperature at $x = 1$ for VHF and VHTC cases, respectively) always attain maximum at the plate itself. From Fig. 9 it is observed that the dimensionless stream function profiles f_2 when $x = 1$ for VHTC case are always convex near the plate.

Fig. 10 shows the variation of dimensionless wall temperature $T_{w2}(x)$ with x for VHTC case. It is observed that when $r = -0.5$, T_{w2} is constant for all x and T_{w2} increases

Table 7
Comparison of results for VHF case and VHTC case

Non-Boussinesq fluid (present study for VHF case)	Non-Boussinesq fluid (present study for VHTC case)
$q_{w1}(x) = x^n$	$h_{w2}(x) = x^r$
$T_{w1}(x) = x^{(2n+1)/4}\theta_1(0)$, $\psi_1(x,\infty) = x^{(2n+3)/4} f_1(\infty)$	$T_{w2}(x) = x^{(2r+1)/2}\theta_2(0)$, $\psi_2(x,\infty) = x^{(r+1)} f_2(\infty)$
Analytical solution for $n = \frac{1}{2}$	Analytical solution for $r = 0$
No multiple solutions	No multiple solutions
No solutions for $n \leqslant -1$	No solutions for $r \leqslant -\frac{3}{4}$
Series solutions for $n = -1 + 2\varepsilon$, $\varepsilon > 0$ $A_1 \approx \sqrt{\pi\varepsilon(1 - 6.5797363\varepsilon)}$ $f_1(\infty) \approx (2 - 9.8696044\varepsilon + 77.8930842\varepsilon^2)/A_1$ $\theta_1(0) \approx 1/A_1$	Series solutions for $r = -0.75 + \varepsilon$, $\varepsilon > 0$ $A_2 \approx \pi\varepsilon(1 - 6.5797363\varepsilon)$ $f_2(\infty) \approx (2 - 9.8696044\varepsilon + 77.8930842\varepsilon^2)/A_2$ $\theta_2(0) \approx 1/A_2$
Series solutions for $n = -0.5 + 2\varepsilon$, $\varepsilon \to 0$ $A_1 \approx \sqrt{0.376526 + 0.922721\varepsilon - 0.982136\varepsilon^2}$ $f_1(\infty) \approx (1.090320 - 1.509365\varepsilon + 3.167386\varepsilon^2)/A_1$ $\theta_1(0) \approx 1/A_1$	Series solutions for $r = -0.5 + \varepsilon$, $\varepsilon \to 0$ $A_2 \approx 0.376526 + 0.922721\varepsilon - 0.982136\varepsilon^2$ $f_2(\infty) \approx (1.090320 - 1.509365\varepsilon + 3.167386\varepsilon^2)/A_2$ $\theta_2(0) \approx 1/A_2$
Asymptotic solutions for $n \to \infty$ $\theta_1(0) \approx 1.286572 n^{-1/4}$, $f_1(\infty) \approx 1.197511 n^{-3/4}$	Asymptotic solutions for $r \to \infty$ $\theta_2(0) \approx 1.170452 r^{-1/2}$, $f_2(\infty) \approx 0.770342 r^{-1}$

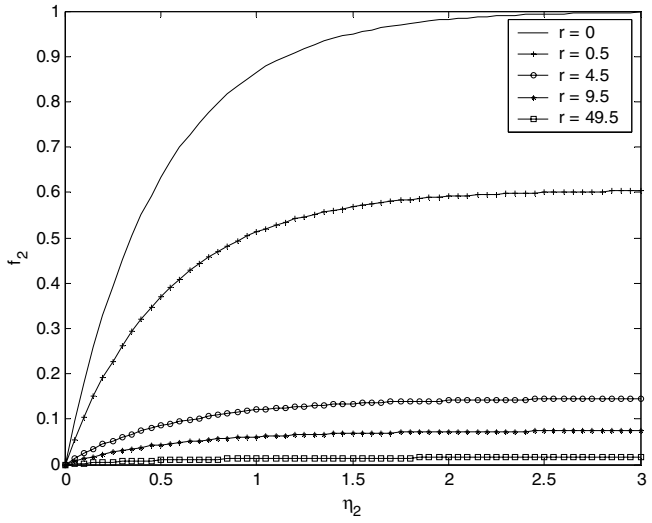

Fig. 9. Plots of f_2 for various values of r (VHTC case).

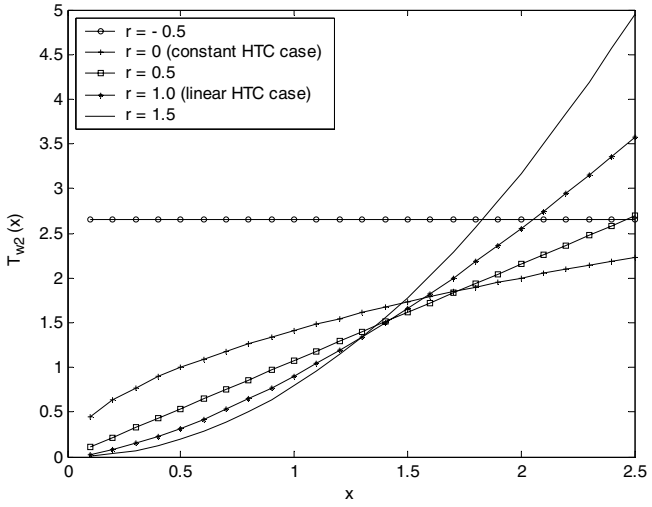

Fig. 10. Variation of dimensionless wall temperature with x for various values of r (VHTC case).

with increasing x for $r > -0.5$ whereas T_{w2} decreases with increasing x for $r < -0.5$.

Variation of dimensionless wall temperatures ($T_{w0}(x) = 1, T_{w1}(x), T_{w2}(x)$) and dimensionless free stream velocity component normal to the plate ($v(x,\infty)$) with x for constant WT, constant HF, and constant HTC cases are shown in Figs. 5 and 6. Noting that in the case of CWT, $T_{w0}(x) = 1$ for all x, it is seen that in the case of CHTC, $v(x,\infty) = -1$ for all x. It is observed that when $x < 0.782758$, $T_{w1}(x)$ for CHF case is greater than $T_{w2}(x)$ for CHTC case whereas when $x > 0.782758$, $T_{w1}(x)$ for CHF case is smaller than $T_{w2}(x)$ for CHTC case. Also,

$$-v(x,\infty)|_{CWT} < -v(x,\infty)|_{CHF} < -v(x,\infty)|_{CHTC}$$

when $x > 0.490294$.

Acknowledgements

The authors wish to express their sincere thanks to an anonymous referee for his valuable comments and suggestions which led to the improvement of the paper.

Appendix A

Solution of Eqs. (13),(14) and (15b,c) *when* $m = -1/2$.

When $m = -1/2$, let $f_0(0) = a$, where a is an arbitrary constant. Now Eqs. (13), (14) and (15b,c), give f_0' and θ_0 which are independent of a. Multiplying Eq. (14) by θ_0' and integrating from η to ∞, we get $(\theta_0')^2 + \frac{1}{4}\theta_0^4 = 0$, which gives $\theta_0(\eta) \equiv 0$. This is in contradiction with Eq. (15b). In the above derivation we assumed $\theta_0'(\infty) = 0$, which follows from the general boundary condition (10b). Hence we conclude there is no physically realistic solution when $m = -1/2$.

References

[1] D.A. Nield, A. Bejan, Convection in Porous Media, second ed., Springer, New York, 1999.
[2] D.B. Ingham, I. Pop (Eds.), Transport Phenomena in Porous Media, Pergamon, Oxford, 1998, vol. II 2002, vol. III 2005.
[3] K. Vafai (Ed.), Handbook of Porous Media, Marcel Dekker, New York, 2000.
[4] I. Pop, D.B. Ingham, Convective Heat Transfer: Mathematical and Computational Modelling of Pergamon, Pergamon, Oxford, 2001.
[5] A. Bejan, A.D. Kraus (Eds.), Heat Transfer Handbook, Wiley, New York, 2003.
[6] D.B. Ingham, A. Bejan, E. Mamut, I. Pop (Eds.), Emerging Technologies and Techniques in Porous Media, Kluwer, Dordrecht, 2004.
[7] A. Bejan, I. Dincer, S. Lorente, A.F. Miguel, A.H. Reis, Porous and Complex Flow Structures in Modern Technologies, Springer, New York, 2004.
[8] Handbook of Chemistry and Physics, 65th ed., CRC Press, Boca Raton, Florida, 1984.
[9] L. Goren, On free convection in water at 4 °C, Chem. Eng. Sci. 21 (1966) 515–518.
[10] D.R. Moore, N.O. Weiss, Non linear penetrative convection, J. Fluid Mech. 61 (1973) 553–581.
[11] B. Gebhart, J.C. Mollendorf, A new density relation for pure and saline water, Deep-Sea Res. 24 (1977) 831–848.
[12] G. Ramanaiah, G. Malarvizhi, A note on the solution of a class of two-point boundary value problems involving a mixed boundary condition, Appl. Math. Lett. 5 (1992) 7–9.
[13] G. Ramanaiah, V. Kumaran, Natural convection about a permeable cone and a cylinder subjected to a radiation boundary condition, Int. J. Eng. Sci. 30 (1992) 693–699.
[14] G. Ramanaiah, V. Kumaran, Convective heat transfer due to a rotating disk subjected to a mixed thermal boundary condition, in: Proceedings of the IMACS 13th World Congress on Computation and Applied Mathematics, Ireland, vol. 2, 1991, pp. 896–897.
[15] J.H. Merkin, Natural-convection boundary-layer flow on a vertical surface with Newtonian heating, Int. J. Heat Fluid Flow 15 (1994) 392–398.
[16] D. Lesnic, D.B. Ingham, I. Pop, Free convection boundary-layer flow along a vertical surface in a porous medium with Newtonian heating, Int. J. Heat Mass Transfer 42 (1999) 2621–2627.

[17] D. Poulikakos, Maximum density effects on natural convection in a porous layer differentially heated in the horizontal direction, Int. J. Heat Mass Transfer 27 (1984) 2067–2075.
[18] D. Poulikakos, Onset of convection in a horizontal porous layer saturated with cold water, Int. J. Heat Mass Transfer 28 (1985) 1899–1905.
[19] K.R. Blake, A. Bejan, D. Poulikakos, Natural convection near 4 °C in water saturated porous layer heated from below, Int. J. Heat Mass Transfer 27 (1984) 2355–2364.
[20] D.B. Ingham, S.N. Brown, Flow past a suddenly heated vertical plate in a porous medium, Proc. Roy. Soc. London A 403 (1986) 51–80.